Journal of Colloid and Interface Science 503 (2017) 39–46

Contents lists available at ScienceDirect

Journal of Colloid and Interface Science

journal homepage: www.elsevier.com/locate/jcis

Regular Article

Importance of crystallinity of anchoring block of semi-solid amphiphilic triblock copolymers in stabilization of silicone nanoemulsions

Trang Huyen Le Kim [a], Hwiseok Jun [a], Yoon Sung Nam [a,b,*]

[a] Department of Materials Science and Engineering, Korea Advanced Institute of Science and Technology, 291 Daehak-ro, Yuseong-gu, Daejeon 34141, Republic of Korea
[b] KAIST Institute for the NanoCentury, Korea Advanced Institute of Science and Technology, 291 Daehak-ro, Yuseong-gu, Daejeon 34141, Republic of Korea

GRAPHICAL ABSTRACT

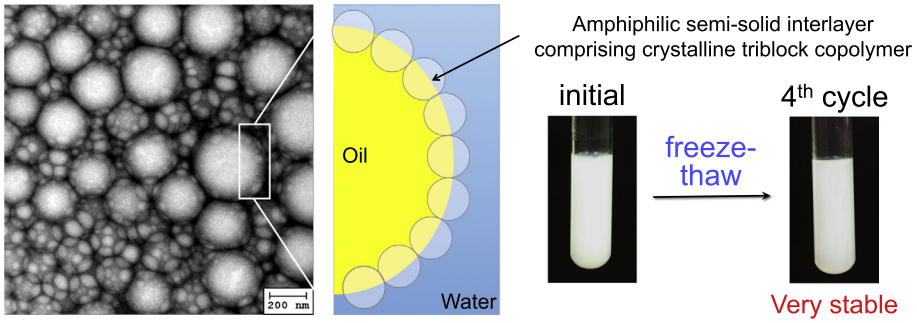

ARTICLE INFO

Article history:
Received 9 March 2017
Revised 23 April 2017
Accepted 25 April 2017
Available online 26 April 2017

Keywords:
Triblock copolymers
Emulsions
Silicone
Dispersion stability
Crystallinity

ABSTRACT

Polymer emulsifiers solidified at the interface between oil and water can provide exceptional dispersion stability to emulsions due to the formation of unique semi-solid interphase. Our recent works showed that the structural stability of paraffin-in-water emulsions highly depends on the oil wettability of hydrophobic block of methoxy poly(ethylene glycol)-*block*-poly(ε-caprolactone) (mPEG-*b*-PCL). Here we investigate the effects of the crystallinity of hydrophobic block of triblock copolymer-based emulsifiers, PCLL-*b*-PEG-*b*-PCLL, on the colloidal properties of silicone oil-in-water nanoemulsions. The increased ratio of L-lactide to ε-caprolactone decreases the crystallinity of the hydrophobic block, which in turn reduces the droplet size of silicone oil nanoemulsions due to the increased chain mobility at the interface. All of the prepared nanoemulsions are very stable for a month at 37 °C. However, the exposure to repeated freeze-thaw cycles quickly destabilizes the nanoemulsions prepared using the polymer with the reduced crystallinity. This work demonstrates that the anchoring chain crystallization in the semi-solid interphase is critically important for the structural robustness of nanoemulsions under harsh physical stresses.

1. Introduction

The dispersions of nano- to micron-scale droplets are stabilized by the thin film of amphiphilic molecules self-assembled at the interface of two immiscible phases via multiple intermolecular interactions, including electrostatic interactions, steric hindrance, the Marangoni effect, and mechanical forces [1–3]. The dispersion or structural stability of emulsions, which can be determined by the variation in the size of droplets, largely depends on the molecular conformation and orientation of emulsifiers at the interface. Among a wide range of amphiphilic molecules, polymeric emulsifiers have gained increasing attention due to their excellent structural and chemical stability, low critical micelle concentration (c.

* Corresponding author at: Department of Materials Science and Engineering, Korea Advanced Institute of Science and Technology, 291 Daehak-ro, Yuseong-gu, Daejeon 34141, Republic of Korea (Y.S. Nam).
E-mail address: yoonsung@kaist.ac.kr (Y.S. Nam).

http://dx.doi.org/10.1016/j.jcis.2017.04.079
0021-9797/

m.c.), facile functionalization, and stimuli-responsive properties [4–9]. Polymeric emulsifiers are particularly effective for suppressing Ostwald ripening, which is the major mechanism of nanoemulsion destabilization [5,10]. The steric hindrance has been considered as the major mechanism of emulsion stabilization by non-ionic polymeric emulsifiers [11]. Accordingly, the deep penetration of an anchoring polymer chain into a dispersed droplet can also appreciably contribute to the stabilization of emulsions through the reduced unfavorable interactions between an anchoring polymer chain and solvent molecules, which in turn facilitate the favorable interaction of a corona polymer chain with the dispersed phase [5,10,12]. Therefore, it is generally believed that the anchoring segment of a polymeric emulsifier needs to be highly soluble in the dispersed phase for the successful stabilization of emulsions, while the corona needs to be more extended toward the aqueous phase.

However, our previous works proposed a counterintuitive concept for emulsion stabilization by non-ionic polymeric emulsifiers via the formation of semi-solid interphase between the immiscible phases [13–17]. The underlying mechanism is similar to the Pickering-like process, which was suggested by Fuller and his colleagues for a graft-type polymeric siloxane [18], although the anchoring block is not soluble in the dispersed phase in our approach. The concept was implemented using methoxy poly (ethylene glycol)-*b*-poly(ε-caprolactone) (mPEG-*b*-PCL), where PCL is insoluble in both of the oil and aqueous phase, as an emulsifier for various oil-in-water (O/W) emulsions. The block copolymer is miscible with a mixture of alcohol and oil at an elevated temperature, but when the solution is dispersed in water, mPEG-*b*-PCL is self-assembled in the dispersed phase, transferred towards the interface, and frozen as a robust semi-solid interphase that effectively stabilizes the emulsions. It was also revealed that the dispersion stability of O/W nanoemulsions prepared using mPEG-*b*-PCL is greatly affected by the type of oils [13]. Stable nanoemulsions were successfully prepared using relatively polar silicone and ester oils, while nanoemulsions of non-polar hydrocarbon oils (e.g., liquid paraffin, dodecene, isopropyl myristate) were very unstable. Our recent work showed that the increased wettability of the hydrophobic block of semi-solid type polymeric emulsifiers can appreciably contribute to the stabilization of nanoemulsions of non-polar oils [16]. However, it is still not fully elucidated which molecular properties of the polymeric emulsifier and their relevant intermolecular interactions determine the successful formation of stable semi-solid interphase that can guarantee emulsion stability.

In this work, we investigated the effects of crystallinity of hydrophobic blocks of amphiphilic triblock copolymers on the colloidal properties of silicone oil nanoemulsions. Triblock copolymers were synthesized by the ring-opening polymerization of ε-caprolactone (CL), forming a hydrophobic block, with polyethylene glycol (PEG) as a hydrophilic block, resulting in poly(ε-caprolactone)-*block*-polyethylene glycol-*block*-poly(ε-caprolactone) (PCL-*b*-PEG-*b*-PCL). To decrease the crystallinity of the hydrophobic block, a small amount of L-lactide (LL) was added as a co-monomer with CL to the hydrophobic blocks, producing poly(ε-caprolactone-*co*-lactide)-*block*-polyethylene glycol-*block*-poly(ε-caprolactone-*co*-lactide) (PCLL-*b*-PEG-*b*-PCLL). The aliphatic polyester used as the hydrophobic block have been widely utilized for pharmaceutical and biomedical applications due to their excellent biocompatibility and biodegradability [19,20]. The molecular weight, chemical composition, and thermal properties of the synthesized triblock copolymers were characterized, and the effects of different hydrophobic blocks on the size distribution, morphology, and dispersion stability of the prepared nanoemulsions were examined to discuss the importance of the crystallinity of the hydrophobic anchoring block in the stabilization of silicone oil nanoemulsions under harsh mechanical stresses generated by repeated freeze-thaw cycles.

2. Experimental section

2.1. Materials

CL (>99%), LL (>98%), PEG (MW = 4.6 kDa), stannous octoate (~95%), dichloromethane (>99.5%), dimethyl sulfoxide (DMSO, >99%), and other organic solvents were purchased from Sigma Aldrich (St. Louis, MO, USA). Phenyl trimethicone (PTM) were obtained from Shin-Etsu Chemical Co., Ltd. (Tokyo, Japan).

2.2. Polymer synthesis

Triblock copolymers of PEG and PCLL were synthesized by ring-opening copolymerization of CL and LL with PEG as the initiator. Briefly, 4 g of PEG were added to a round bottom flask and vacuum drying at 90 °C for 3 h to remove absorbed humid and water vapor. Then, 4 g of a mixture of CL and LL with pre-determined weight ratios (0, 5, and 10 wt.% of LL) and 40 mg stannous octoate were added to the flask. The mixture was dried in vacuum for 1 h. Then, the flask was sealed, and the temperature was increased to 130 °C. The reaction was kept for 24 h. After finishing the reaction, the mixture was dissolved in dichloromethane, followed by the addition of chilled methanol (−20 °C) to precipitate the produced polymers. The precipitates were collected by centrifugation, and the recrystallization procedures in methanol were repeated three times. The polymer precipitates were then dried in vacuum for 48 h.

2.3. Polymer characterization

The molecular weights of synthesized polymers were analyzed using gel permeation chromatography (GPC). A high performance liquid chromatography (HPLC) system composed of Agilent 110 series (Agilent Technologies, Palo Alto, CA, USA) and a refractive index detector was operated at 1.0 mL min^{-1} using a series of three PL gel columns (300 × 7.5 mm, pore sizes = 10^3, 10^4, and 10^5 Å) as size exclusion columns. Tetrahydrofuran was used as an isocratic mobile phase, and monodisperse polystyrenes (Polysciences, Inc., Warrington, PA, USA) were used as calibration standards. Chemical structure and chemical composition were analyzed using ^{1}H nuclear magnetic resonance (NMR, Bruker) at 25 °C operating at 300 MHz using $CDCl_3$ as a solvent. Chemical shifts were measured in parts per million (ppm) using tetramethylsilane as an internal reference. Thermal properties of block copolymers were analyzed using differential scanning calorimetry (DSC 204 F1 Phoenix, Netzsch-Gerätebau GmbH, Selb, Germany). Two cycles of heating and cooling scans were run between −50 °C and 200 °C at a scan rate of 10 °C min^{-1}. Experiments were repeated three times. Data from the second heating were analyzed, and the enthalpy of endothermic processes was determined. The degree of crystallinity was calculated from the melting enthalpy of the second heating using the Eq. (1).

$$\chi_c(\%) = \frac{\Delta H_m}{w_{PEG}\Delta H^o_{mPEG} + w_{PCL}\Delta H^o_{mPCL} + w_{PLL}\Delta H^o_{mPLL}} \times 100 \quad (1)$$

where χ_c is the degree of crystallinity of the copolymer (%), ΔH_m is the melting enthalpy of the copolymer (J g^{-1}), w_{PEG}, w_{PCL}, and w_{PLL} are the weight fractions of PEG, PCL, and PLL in the copolymer, respectively, ΔH^o_{mPEG}, ΔH^o_{mPCL}, and ΔH^o_{mPLL} are the melting enthalpies of crystalline PEG, PCL, and PLL, which are 205, 139, and 93.7 J g^{-1}, respectively.

2.4. Preparation of polymeric micelles and nanoemulsions

For polymeric micelles, ten milligrams of polymer were dissolved in DMSO, and then the solution was dropped slowly into deionized water with magnetic stirring at 600 rpm. DMSO was then removed by dialysis against deionized water through a Spectra/Por RC dialysis membrane (MWCO = 12–14 kDa) for 24 h. PTM nanoemulsions were prepared using triblock copolymers as followed. Ten milligrams of polymer and 100 mg of PTM were dissolved completely in 1 mL acetone. The organic solution was then dropped slowly into 10 mL of deionized water with magnetic stirring at 600 rpm. Acetone was completely evaporated for 12 h at room temperature.

2.5. Characterization of polymeric micelles and nanoemulsions

The size distributions of the prepared polymeric micelles and nanoemulsions were measured using dynamic light scattering (DLS) at 25 °C with ELSZ-1000 (Otsuka Electronics Co., Ltd., Japan). The c.m.c. was determined by adding pyrene into a series of polymeric micelle solutions at different concentrations, then fluorescent absorption of the mixtures were measured using a fluorescence spectrophotometer F7000 (Hitachi, Japan) with a quartz cell. Fluorescence spectra were recorded from 350 nm to 450 nm with excitation at 332 nm. Scan speed was 240 nm min^{-1}, and the slit width was set at 5 nm for both of excitation and emission. The peak intensities at 372 nm and 383 nm were collected, and their ratios (I_{372}/I_{383}) were recorded as a function of the polymer concentration. Transmission electron microscopy (TEM) specimens were prepared by mixing 10 μL of nanoemulsions with 10 μL of 2 wt.% uranyl acetate and then diluting the mixture ten times with deionized water. Five microliters of the diluted solution were dropped on a carbon-coated copper grid (Ted Pella, Inc., Redding, CA, USA), followed by air drying. The samples were observed using JEM 3010 (JEOL, Akishima, Japan) operated at 300 kV. Emulsions samples prepared for DSC analysis were done by freeze-drying 5 mL of emulsions, and the analysis was done as described previously. The dispersion stability of nanoemulsions was examined by monitoring the changes in the size distribution of nanoemulsions incubated at 37 °C for one month. Repeated freeze-thaw cycles were also applied to the nanoemulsions: −20 °C for 10 h and room temperature for 4 h.

3. Results and discussion

3.1. Synthesis and characterization of triblock copolymers

Triblock copolymers, PCLL-*b*-PEG-*b*-PCLL, were synthesized by ring-opening copolymerization of a mixture of CL and LL, initialized by the two hydroxyl end groups of PEG, as schematically described in Fig. 1A. Due to the two hydroxyl end groups of PEG, CL and LL propagated along both directions with the units randomly mixed, resulted in the formation of triblock copolymers with PEG in the middle and PCL or PCLL at the both ends. Three different weight ratios (0, 5, and 10 wt.%) of LL in the hydrophobic block were used to investigate the effect of LL portions. The average molecular weights of the synthesized polymers were analyzed using GPC (Table 1 and Fig. S1). The number average molecular weights of 0, 5, 10 wt.% LL fed (denoted 'TP0', 'TP5', and 'TP10') were 14.6, 18.8, and 18.6 kDa, respectively. The chemical structure of the synthesized polymers was analyzed using ^{1}H NMR spectroscopy (Fig. 1B and Fig. S2). The NMR peak numbers 1, 2, 3, and 4 correspond to the hydrogen in the CL unit, the peak number 5 to the hydrogen of PEG, and the peak numbers 6 and 7 to the hydrogen in the LL units. The appearance of peak numbers 6 and 7 confirmed the successful incorporations of LL to the resulting copolymers. The molar and weight ratios of monomeric units, calculated from ^{1}H NMR spectra, are summarized in Table 1. The actual LL contents, determined from NMR, were 0, 6.6, and 10.16 wt.%, which were close to the fed ratios, indicating the successful synthesis of the triblock copolymers. The numbers of each monomer unit were also calculated and added to the sample names in Table 1. Thermal properties of the triblock copolymers, determined by DSC, are shown in Fig. 1C,D, and Table 2. In the endothermic DSC curves, as the LL contents were increased, the melting peak was shifted to the left, and the melting temperature and enthalpy were decreased. The calculated degree of crystallinity was decreased from 60% (TP0) to 57% (TP5) and 50% (TP10). The decreased crystallinity was ascribed to the presence of intercalated LL in the PCL chain packing.

3.2. Micelle-like aggregates of triblock copolymers

The self-assembly behaviors of the triblock copolymers were examined in terms of dynamic size distribution and c.m.c. The synthesized polymer was dissolved in DMSO, and the polymer solution was added dropwisely into deionized water, immediately generating polymeric micelles. Due to the hydrophobicity of the PCL and PCLL blocks, they were aggregated into the core and forced to expose the hydrophilic PEG blocks outward to the aqueous phase, forming micelles-like polymeric aggregates [8]. Pyrene was added to the polymer micellar solution, and the fluorescence emission spectra were obtained. The c.m.c. was determined from a drastic change in the intensity ratio caused by the formation of hydrophobic domains, to which pyrene is partitioned. In Fig. 2A, the ratio of pyrene fluorescence intensities at 372 nm and 383 nm in the triblock copolymer solution was decreased from 8.2×10^{-4} g L^{-1} to 4.7×10^{-4} g L^{-1}. These values correspond to the typical range of c.m.c. of the same type of amphiphilic block copolymers [16,17]. The c.m.c. was decreased as the fed LL was increased from 0 (TP0) to 5 (TP5) and to 10% (TP10) (Fig. 2B). The size distributions of the polymeric micelles were also determined using DLS (Fig. 2C). The average hydrodynamic diameter was decreased from 89 nm (TP0) to 71 nm (TP5) and to 61 nm (TP10) as the portion of LL was increased. The results indicate that the reduced crystallinity by the addition of LL to the hydrophobic block allowed the polymer chain to self-assemble at a lower concentration and produce smaller micelle-like aggregates due to the increased mobility of the hydrophobic polymer chain.

3.3. Crystallinity of triblock copolymers wetted by silicone oil

To determine the crystallinity of the synthesized polymers wetted by PTM, we dispersed the polymers in the oil with magnetic stirring at 600 rpm and incubated at 80 °C for 24 h. At the elevated temperature, the melted polymer and oil were miscible to form a homogeneous, transparent phase. However, as the temperature was dropped to an ambient temperature, thermally induced solid-liquid phase separation occurred [20,21]. After the polymer mass was solidified and separated from the oil phase, the thermal properties of the oil-wetted polymers were analyzed using DSC. Endothermic melting peaks were splitted for all of the polymers, as observed for PCL homopolymers [17]. This phenomenon can be ascribed to the heterogeneous nucleation of two crystalline phases in the PCL block due to different spatial confinement [22]. The decreased melting temperatures and enthalpies were observed as the LL portion was increased, similar as the dried polymer powders, although the oil-wetted polymers had much lower melting temperatures and crystallinity (Fig. 3 and Table 2). Moreover, as the LL portion was increased, the degree of crystallinity of the oil-wetted polymers exhibited a larger shift compared to that of

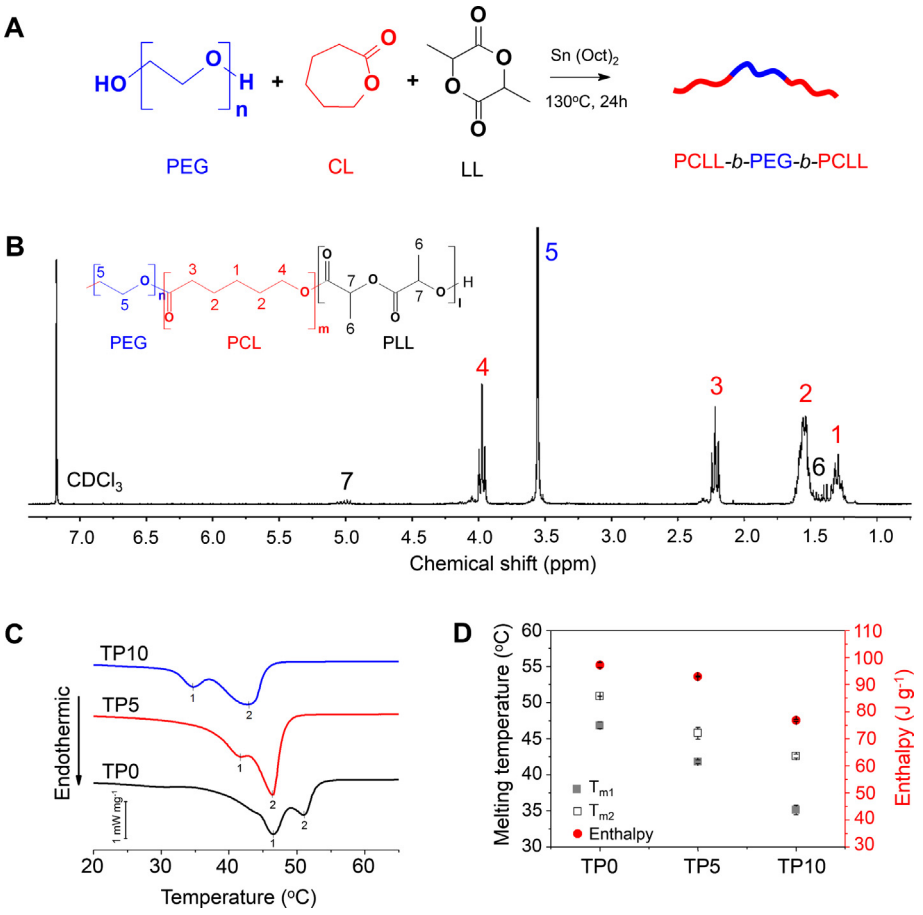

Fig. 1. Synthesis and characterization of PCLL-PEG-PCLL triblock copolymers. (A) Schematic synthetic procedures of the triblock copolymers. (B) ^{1}H NMR spectrum of TP10 with the inserted image of the chemical formula of three monomeric units. Full molecular structure and ^{1}H NMR spectra of the triblock copolymers are presented in Fig. S2. (C) DSC curves from the second heating of the synthesized copolymers. (D) Melting temperature and enthalpy of the synthesized copolymers determined from (C).

Table 1
Molecular weights and composition of the synthesized triblock copolymers.

	Sample name with unit number[a]	M_n[b]	M_w[b]	PDI[b]	Molar ratio[c]			Weight ratio[c]			wt.% LL[c]
					PEG	PCL	PLL	PEG	PCL	PLL	
TP0	PCL_{42}-PEG_{117}-PCL_{42}	14,656	19,098	1.303	1	0.71	0	1	1.85	0	0
TP5	$PCLL_{52}$-PEG_{167}-$PCLL_{52}$	18,889	21,122	1.118	1	0.59	0.03	1	1.54	0.11	6.6
TP10	$PCLL_{62}$-PEG_{113}-$PCLL_{62}$	18,636	23,242	1.247	1	1.00	0.09	1	2.59	0.29	10.16

[a] Calculated from M_n and molar ratio.
[b] Calculated from GPC chromatogram.
[c] Calculated from ^{1}H NMR spectra.

Table 2
Thermal properties of the synthesized triblock copolymers, oil-wetted polymer, and nanoemulsions analyzed from DSC.

Type	Denote	Melting peak 1 (°C)	Melting peak 2 (°C)	Enthalpy (J g^{-1})	Degree of crystallinity (%)
Polymer	TP0	46.86 ± 0.48	50.92 ± 0.02	97.15 ± 0.91	59.91 ± 0.56
	TP5	41.82 ± 0.25	45.78 ± 0.81	92.90 ± 0.14	57.34 ± 0.09
	TP10	35.13 ± 0.66	42.60 ± 0.28	76.78 ± 0.39	50.30 ± 0.25
Oil-wetted polymer	PTM-TP0	42.06 ± 0.15	48.51 ± 0.36	77.06 ± 0.54	47.52 ± 0.33
	PTM-TP5	36.77 ± 0.35	42.91 ± 0.36	64.41 ± 1.05	39.75 ± 0.65
	PTM-TP10	28.17 ± 0.41	36.72 ± 0.46	47.41 ± 0.45	31.07 ± 0.29
Emulsions	PTM-TP0	43.00 ± 0.20	47.40 ± 0.62	18.52 ± 0.38	11.42 ± 0.23
	PTM-TP5	37.53 ± 0.35	41.70 ± 0.30	17.55 ± 0.31	10.83 ± 0.19
	PTM-TP10	31.27 ± 0.31	37.67 ± 0.25	15.01 ± 0.40	9.83 ± 0.26

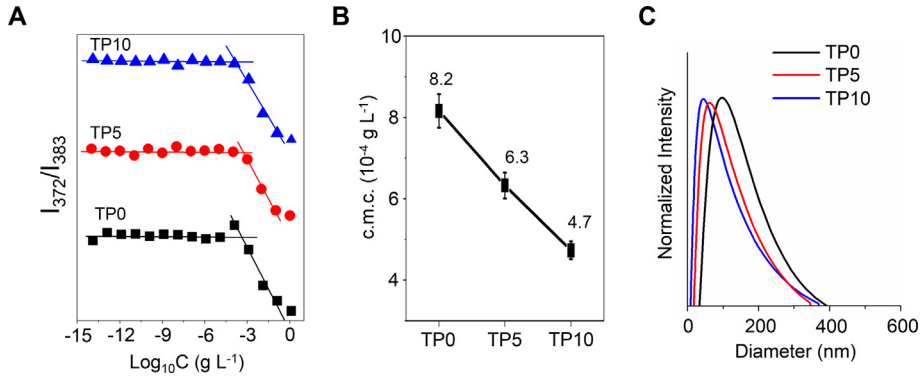

Fig. 2. Characterization of polymeric micelles formed by self-aggregation of the synthesized triblock copolymers. (A) Fluorescence intensity ratios from the fluorescence spectra of pyrene in the polymeric micelle solutions as a function of polymer concentration. (B) c.m.c. values of the triblock copolymer calculated from (A). (C) Hydrodynamic size distributions of the polymeric micelles measured using DLS.

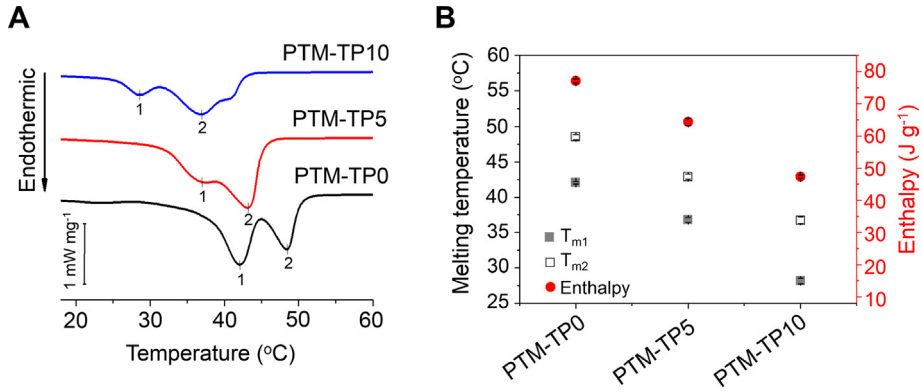

Fig. 3. Thermal properties of the triblock copolymers wetted by silicone oil. (A) DSC curve from the second heating scan of the polymers immersed in PTM. (B) Melting temperature and enthalpy measured from (A).

dry polymers, as summarized in Table 2. The results indicate that the incorporation of LL into the hydrophobic block effectively reduced the crystallinity, which in turn allowed higher chain mobility of the polymer in the organic phase.

3.4. Preparation of silicone oil emulsions

Next, we prepared silicone oil-in-water nanoemulsions using the synthesized triblock copolymers as emulsifiers and examined the effect of the crystallinity of the hydrophobic blocks on the dispersion stability of nanoemulsions. A mixture of PTM and PCL-*b*-PEG-*b*-PCL (or PCLL-*b*-PEG-*b*-PCLL) was completely dissolved in acetone at room temperature. The homogeneous mixture solution of PTM and polymer in acetone was then added to deionized water with magnetic stirring at 600 rpm, resulting in immediate dispersion into nanoscale droplets through the phase inversion mechanism [16,17]. As the polar organic solvent in the droplets quickly diffuses out to the aqueous phase, the polymer chains rapidly migrate towards the O/W interface and be solidified at the droplet surface, forming a semi-solid interphase on the surface of silicone oil droplets. In the meanwhile, the hydrophilic PEG block can stretch out to the aqueous phase to stabilize the droplets via steric hindrance. If the triblock copolymers are irreversibly frozen before they reach the O/W interface, macroscopic phase separation between the polymer and oil in the organic phase can occur, eventually failing in the stabilization of nanoemulsions [14]. Therefore, the formation of a stable interphase highly depends on the kinetics of solidification of the hydrophobic block, which can be modulated by the chain mobility and solvent miscibility of the polymer.

3.5. Size distributions of nanoemulsions

The size distribution of nanoemulsions prepared using the triblock copolymers was determined using DLS, as shown in Fig. 4A. Although all of the prepared nanoemulsions exhibited similar size distributions, the mean hydrodynamic diameter was decreased with the increased LL portion: 236 ± 98, 222 ± 96, and 194 ± 80 nm for TP0, TP5, and TP10, respectively (Fig. 4B). This result is inconsistent with that of mPEG-*b*-PCLL diblock copolymers reported in our recent paper, where the droplet size of PTM nanoemulsions was slightly increased as more LL was incorporated to the hydrophobic block [16]. The difference in the size distributions of nanoemulsions between the diblock and triblock copolymers can be explained by the effect of molecular structures on the chain mobility in the organic phase. In the diblock copolymer, mPEG has a free end, allowing its flexibility and mobility in an organic phase comprising polar oils, so the impact of the oil-hydrophobic block interactions on the formation of nanoemulsions can be limited. However, in the triblock copolymer, the chain mobility of PEG is substantially restricted by the hydrophobic blocks tethered at the both ends, and thus the oil wettability of the hydrophobic block determines how quickly the polymer chain migrates towards the interface and changes its chain conformation to expose the hydrophilic block to the aqueous phase. Hence, the increased chain mobility (reduced crystallinity) by the addition of LL to the hydrophobic block allowed TP10 to form smaller nanoemulsions due to the kinetically faster polymer migration to the interface than solid-liquid phase separation. In addition, TP10 could have slower solidification (crystallization) at the interface compared to the more crystalline polymers (TP0 and TP5).

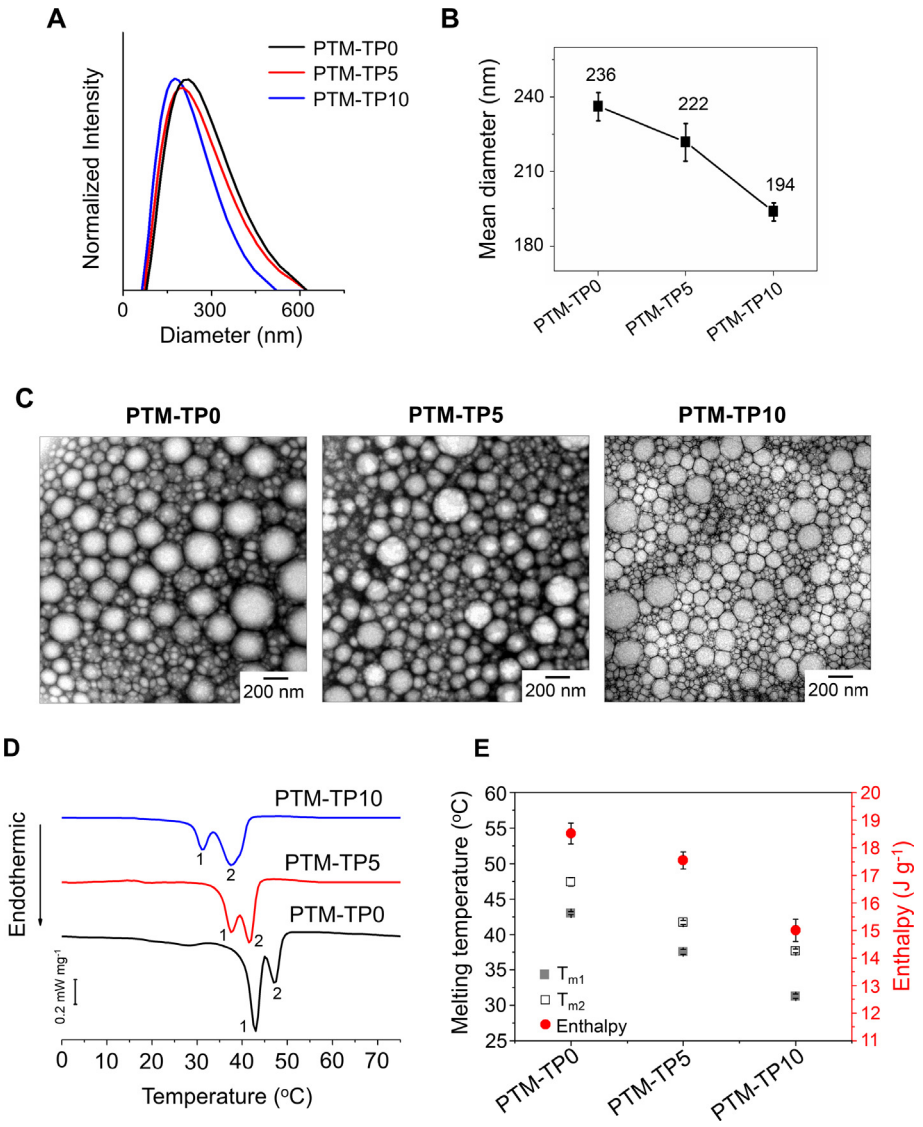

Fig. 4. Properties of silicone oil emulsions stabilized with the triblock copolymers. Hydrodynamic size distributions (A) and mean diameters (B) of PTM nanoemulsions measured using DLS. TEM images of PTM nanoemulsions (C), DSC curves from the second heating scan of freeze-dried emulsions (D) and melting temperatures and enthalpy values measured from the DSC curves (E).

3.6. Morphologies of nanoemulsions

The morphologies of the nanoemulsions were analyzed using TEM, as shown in Fig. 4C. All of the nanoemulsions had a spherical shape with a smooth and homogeneous surface morphology. The surface boundary of the nanoscale droplets, PTM-TP0 and PTM-TP5, does not seem to be deformable despite the high density of nanoemulsions on the TEM grid, indicating that the triblock copolymers formed a very solid film on the surface of droplets [13,15]. In addition, PTM-TP0 nanoemulsions exhibited distinctive, protruded structures on the emulsion surfaces, which indicates the phase separation of the polymer in the organic phase during the formation of nanoemulsions [13]. In contrast, the PTM-TP10 nanoemulsions had relatively smooth, deformable surface morphology, which can be also interpreted by the slower kinetics of interfacial solidification of the polymer. When mPEG-*b*-PCLL was used as an emulsifier, the surface of all of the prepared nanoemulsions was very smooth and thin, irrespective of the composition of the hydrophobic block [16]. It was attributed to the relatively slow solidification of the diblock copolymers in PTM, which allows the polymer chains to migrate to the interface and form a thin polymer interphase on the surface of nanoemulsions. However, even the same polymer produced a completely different surface morphology when ethanol was used as a water miscible solvent instead of acetone. Ethanol is a non-solvent for aliphatic polyesters, so high-pressure homogenization at a high temperature (80 °C) was required to generate PTM nanoemulsions stabilized by mPEG-*b*-PCL [13]. The produced nanoemulsions were very stable, but they had a very rough and protruded morphology similar as PTM-TP0 (and PTM-TP5). Therefore, the results support the idea that solid-liquid phase separation can first occur in the organic phase and then induce the formation of amphiphilic nanoscale structures in the semi-solid interphase, resulting in unique patterns on the surface of oil droplets [21,22].

3.7. Crystallinity of nanoemulsions

Nanoemulsions were freeze-dried for DSC analysis as shown in Fig. 4D,E and Table 2. As the LL content was increased, the melting temperatures of nanoemulsions were decreased, as observed for

the dried and oil-wetted polymers. The melting temperatures of nanoemulsions were more similar as those of the oil-wetted polymer (Table 2). The degree of crystallinity was decreased from 60% in TP0 to 11% in PTM-TP0 and from 50% in TP10 to 9.8% in PTM-TP10. The results indicate that the reduced crystallinity is mainly mediated by the wetting of the polymers by silicone oil.

3.8. Dispersion stabilities of nanoemulsions

The long-term dispersion stability of the nanoemulsions was examined at 37 °C for one month. The nanoemulsions were incubated without using any additional agents, such as thickeners and organic solvents, and applying further mechanical agitation. Although some fluctuation in the hydrodynamic size of droplets was observed, there was no significant variation in the mean hydrodynamic diameter, which was in the range of 200–250 nm (Fig. 5A). The smallest droplet size of nanoemulsions stabilized with TP10 was maintained throughout the incubation period. The nanoemulsions were also exposed to a cyclic freezing-thawing condition, which generates very harsh physical stresses on the interfaces of nanoemulsions [16,17,23,24]. The nanoemulsions were frozen at – 20 °C for 10 h and thawed at room temperature for 4 h. The cyclic procedures were repeated four times, and the changes in the hydrodynamic size were monitored using DLS. The PTM-TP10 nanoemulsions started to show macroscopic phase separation just after the first cycle, while the TP0 and TP5 nanoemulsions were very stable during the four cycles despite slight increase in the mean diameter (Fig. 5B). The hydrodynamic diameter of PTM-TP10 was increased to microns after the second cycle, and the nanoemulsions were destroyed to generate micron-sized particles (Fig. 5C and D) and underwent clear phase separation (Fig. 5E and F). The dashed circle in Fig. 5F indicates the creaming of nanoemulsions generated by the coarsening processes, presumably Ostwald ripening and coalescence. These results indicate that the structural stability of nanoemulsions is highly affected by the crystallinity of the triblock copolymers, which could be a key factor for the stabilization of nanoemulsions against mechanical stresses because other properties of the polymers tested in this work were very similar with each other.

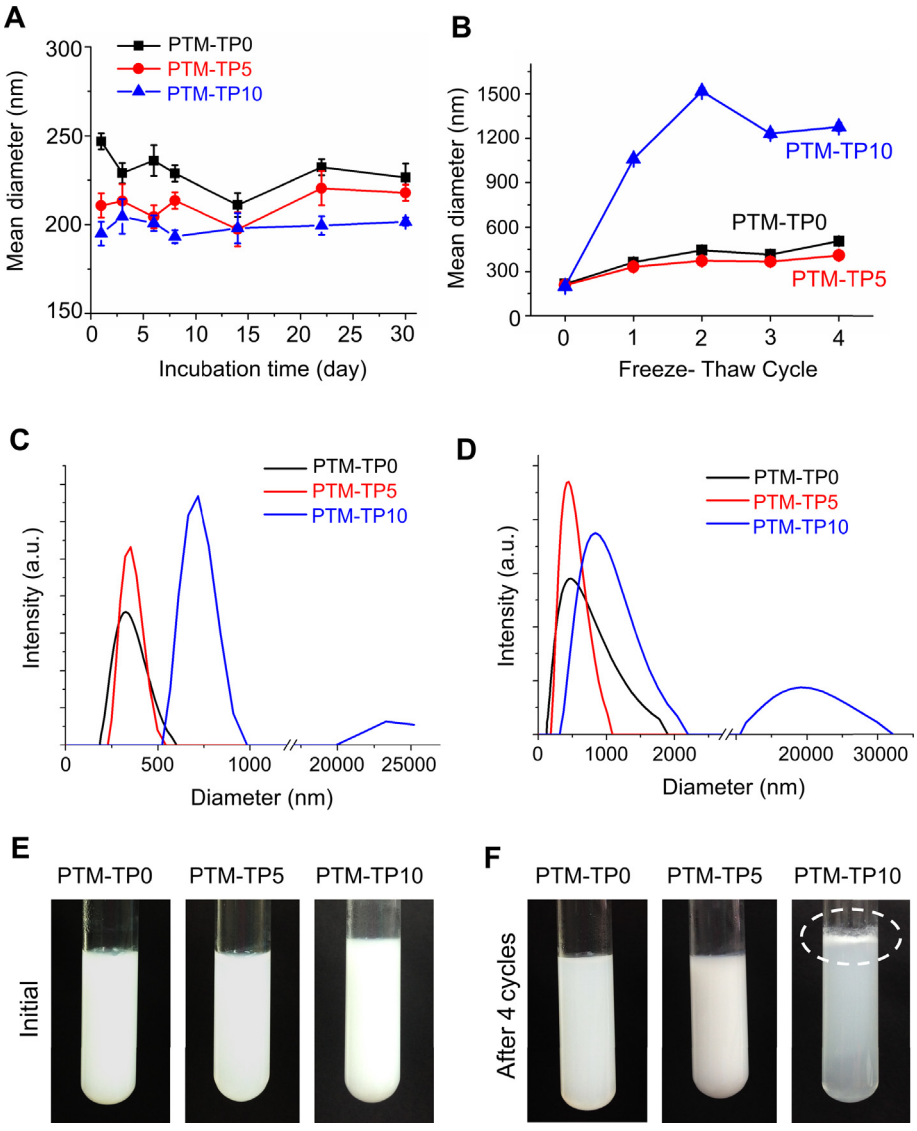

Fig. 5. Dispersion stability of PTM nanoemulsions. (A) Time-course variations of the hydrodynamic diameter at 37 °C for 30 days. (B) Variations in the hydrodynamic diameter through the freeze- thaw cycles between −20 °C and 25 °C. Size distributions after 1 cycle (C) and 4 cycles (D). Photographs of nanoemulsion samples at the initial condition (E) and after four cycles (F).

4. Conclusion

This work demonstrated the impact of crystallinity of amphiphlic triblock copolymers on the structural stability of silicone oil-in-water nanoemulsions under harsh physical stresses. The nanoemulsions were prepared using PCL-*b*-PEG-*b*-PCL as an emulsifier forming a robust semi-solid interphase [13–15]. The crystallinity of the hydrophobic block of PCL-*b*-PEG-*b*-PCL was decreased when CL was co-polymerized with a small amount of LL (less than 10 wt.%) to produce PCLL-*b*-PEG-*b*-PCLL. As the crystallinity of polymer chains was decreased, both of the hydrodynamic size and c.m.c. of polymeric micelles were decreased. As the polymeric micelles were kinetically frozen during the dispersion of water-miscible solvents into water, the highly crystalline polymer might generate the nuclei too quickly due to the precedent phase separation and do not allow the formation of a compact core structure. The addition of LL to the hydrophobic block of the triblock copolymers also decreased the hydrodynamic droplet size of nanoemulsions, while no significant changes were observed for diblock copolymers with similar chemical compositions, which indicates the importance of molecular structures, particularly the mobility and accessibility of PEG chains. Our previous work demonstrated that the use of PCLL as a hydrophobic block is advantageous for the stabilization of nanoemulsions of non-polar hydrocarbon oil, such as paraffin oil, compared to highly crystalline PCL, while both of them exhibited no significant differences for silicone oil [16]. However, in this contribution, we reached the new conclusion that the crystallinity of the hydrophobic block is critically important for the robustness of the semi-solid interphase formed on the surface of silicone oil. We expect that our findings will provide a guideline for the selection of appropriate anchoring segment of a polymeric emulsifier for practical applications where various types of oils, even their mixtures, are used.

Acknowledgements

This study was supported by a grant of the Korea Healthcare Technology R&D Project, Ministry of Health & Welfare, Republic of Korea (Grant No.: HN12C0064).

Appendix A. Supplementary material

Supplementary data associated with this article can be found, in the online version, at http://dx.doi.org/10.1016/j.jcis.2017.04.079.

References

[1] S.I. Karakashev, E.D. Manev, R. Tsekov, A.V. Nguyen, J. Colloid Interf. Sci. 318 (2008) 358–364.
[2] I.B. Ivanov, P.A. Kralchevsky, Colloids Surf., A 128 (1997) 155–175.
[3] P.J. Wilde, Curr. Opin. Colloid Interf. Sci. 5 (2000) 176–181.
[4] A.M. Mathur, B. Drescher, A.B. Scranton, J. Klier, Nature 392 (1998) 367–370.
[5] Th.F. Tadros, A. Vandamme, B. Levecke, K. Booten, C.V. Stevens, Adv. Colloid Interf. Sci. 108–109 (2004) 207–226.
[6] M. Bobin, V. Michel, M. Martini, Colloids Surf., A 152 (1999) 53–58.
[7] T.J. Barnes, C.A. Prestidge, Langmuir 16 (2000) 4116–4121.
[8] Y.S. Nam, H.S. Kang, J.Y. Park, T.G. Park, S.H. Han, I.S. Chang, Biomaterials 24 (2003) 2053–5059.
[9] J. Yeom, Y.S. Nam, Colloid Polym. Sci. 290 (2012) 839–845.
[10] S. Liu, S.P. Armes, Curr. Opin. Colloid Interf. Sci. 6 (2001) 249–256.
[11] G.C. March, D.H. Napper, J. Colloid Interf. Sci. 61 (1977) 383–387.
[12] Y. Sela, S. Magdassi, N. Garti, Colloid Polym. Sci. 272 (1994) 684–691.
[13] Y.S. Nam, J.W. Kim, J. Shim, S.H. Han, H.K. Kim, Langmuir 26 (2010) 13038–13043.
[14] Y.S. Nam, J.W. Kim, J. Shim, S.H. Han, H.K. Kim, J. Colloid Interf. Sci. 351 (2010) 102–107.
[15] Y.S. Nam, J.W. Kim, J. Park, J. Shim, J.S. Lee, S.H. Han, Colloids Surf., B 94 (2012) 51–57.
[16] T.H. Le Kim, H. Jun, J.S. Kim, Y.S. Nam, J. Colloid Interf. Sci. 443 (2015) 197–205.
[17] H. Jun, T.H. Le Kim, S.W. Han, M. Seo, J.W. Kim, Y.S. Nam, Colloid Polym. Sci. 293 (2015) 2949–2956.
[18] J.W. Anseth, A. Bialek, R.M. Hill, G.G. Fuller, Langmuir 19 (2003) 6349–6356.
[19] M.C. Serranoa, R. Pagania, M. Vallet-Regıb, J. Peñab, A. Rámilab, I. Izquierdob, M.T. Portolésa, Biomaterials 25 (2004) 5603–5611.
[20] Y.S. Nam, K.J. Kim, H.S. Kang, T.G. Park, S.H. Han, I.S. Chang, J. Appl. Polym. Sci. 89 (2003) 1631–1637.
[21] Y.S. Nam, T.G. Park, Biomaterials 20 (1999) 1783–1790.
[22] Y.S. Nam, T.G. Park, J. Biomed. Mater. Res. 47 (1999) 8–17.
[23] Y. Suzuki, H. Duran, W. Akram, M. Steinhart, G. Floudas, H.J. Butt, Soft Matt. 9 (2013) 9189–9198.
[24] F. Donsi, Y. Wang, Q. Huang, Food Hydrocoll. 25 (2011) 1327–1336.